DOR: 20.1001.1.2322388.2019.7.4.6.4

Research Paper

Fabrication of anodic aluminium oxide template and the generation of magnetic Co nanowires within it

Masoud Soltani[1], Reihaneh Aliramezani[1], Saeed Akhavan[1*], Zeinab Erfani Gahrouei[1], Mohammad Noormohammadi[2]

1. *Department of Materials Engineering, Isfahan University of Technology, Isfahan, Iran*

2. Department of Physics, Kashan University, Kashan, Iran

ARTICLE INFO

Article history:

Received 11 December 2018
Accepted 2 February 2019
Available online 1 November 2019

Keywords:
Al alloy
Anodizing
Nanowires
Electrodeposition
Coercivity

ABSTRACT

Among nanostructured materials, magnetic nanowires have been heeded because of their high shape anisotropy and their easy fabrication methods. Electrochemical deposition on the anodic aluminium oxide (AAO) is one of the best methods to grow different nanowires. In this paper, the AAO was fabricated on the 1100 Al alloy substrate by hard anodizing in 0.3 M oxalic acid solution. Then, a barrier layer thinning process was carried out for the electrodeposition process. A pulsed electrodeposition process was used to fill the nano-pores. According to this method, cobalt nanowires were grown in the nano-holes. Structural, crystalline, and magnetic properties of the samples were evaluated using field emission scanning electron microscopy (FESEM), X-ray diffraction (XRD), and vibrating sample magnetometer (VSM), respectively. The results showed that nanowires have a diameter of 87 nm and crystalline structure with crystalline plates in directions (100), (002), and (110). A coercivity value of 600 Oe was obtained for nanowires, which is several times larger than cobalt bulk.

[*] **Corresponding Author:**
E-mail: s.a.metallurg@gmail.com

1. Introduction

Magnetic nanowires have been widely investigated not only due to their intriguing magnetic properties but also for their potential applications in ultra-high density data storage and spintronics [1]. Several kinds of methods can be used to fabricate nanowires, such as lithographic patterning and template synthesis [2, 3]. One of the most applicable templates for the growth of nanowires is the AAO (anodic aluminium oxide) template [4-7]. Many studies have been conducted on the AAO fabrication at different voltages and temperatures [8-10]. It was reported that one of the major problems of using hard anodizing for template fabrication is the burning of the sample during this process due to its high voltage [11, 12]. But it can be prevented by the use of mild anodizing before hard anodizing [13]. There are different ways to grow nanowires, like CVD (chemical vapor deposition), electroless and electrochemical deposition [14-16]. Among these methods, the electrodeposition process is widely used due to its easy fabrication as well as its ability to control the composition and crystallinity of nanowires [17]. But an important issue in these studies is the barrier layer thickness of AAO layers [18, 19]. This layer can prevent the proper growth of the nanowires during the electrodeposition process due to its insulating nature [20]. Several researches have been done on the growth of different nanowires such as nickel, iron, silver, and cobalt within the AAO by the electrochemical deposition method [21]. Meanwhile, cobalt nanowires have been much more interesting because of the high magneto-crystalline anisotropy constant of bulk hcp cobalt and also the competition between shape and magneto-crystalline anisotropy of these nanowires [22]. In previous works, in order to appropriate the growth of cobalt nanowires on the AAO template, after a two-step anodizing process, the barrier layer is removed by chemical immersion. Moreover, the anodizing process is usually done on pure Al, which is not interesting for industrial applications such as aviation. Consequently, using magnetic properties of grown nanowires in Al alloys is more interesting for use in industrial applications [21, 23, 24].

The aim of this research was to achieve the appropriate AAO template by using the hard anodizing process on 1100 Al alloy without post chemical immersion and then using this template for the growth of cobalt nanowires by an electrochemical deposition method. In addition, the produced nanowires were characterized by FESEM, XRD, and VSM.

2. Experimental procedure

In this research, disc-shaped samples of 1100 Al alloy with diameter and thickness of 12 mm and 1 mm respectively and also chemical composition (wt%) of 0.62% Si, 0.07% Fe, 0.15% Cu, 0.03% Mn, 0.02% Zn and balance Al were prepared. All the samples were degreased in acetone and then electropolished in a 1:4 volume mixture of perchloric acid and ethanol (Fig. 1).

Templates preparation for the growth of nanowires was carried out using the anodizing process in 0.3 M oxalic acid solution (according to Fig. 2). For anodizing process, a mild anodizing with a voltage of 40V was initially applied for 10 minutes to form a protective layer of alumina on the samples (a-b). This layer protects the samples and prevents the burning of them at high voltages and currents of hard anodizing [13]. Then the voltage was increased to 130 V (hard anodizing voltage) with the rate of 0.4 V/S (b-c) and kept at this voltage for 50 minutes (c-d). Ultimately, the voltage was reduced after the 2400s to decrease the thickness of the barrier layer (d-e). In this process, the cathode was graphite, and the anode-cathode distance of 2.5 cm was selected. The temperature of the solution was kept at 0 °C during the anodizing.

For the growth of the nanowires, an electrodeposition technique using pulsed voltage (Fig. 3) in 0.3 M cobalt sulfate and 40 g/L boric acid solution was used. Finally, the samples were immersed in a 0.3 M sodium hydroxide solution for 40 minutes to release the nanowires after the growth process. In order to investigate the morphology of samples, field emission scanning electron microscopy (FESEM-Hitachi S4160 Cold Field Emission) was employed. The elemental distribution was examined using energy-dispersive X-ray spectroscopy (EDS) detector. The microstructure of Co nanowire arrays was studied by using an X-ray diffraction device (XRD - Philips XPERT-XL30) with radiation of Kα Cu ($\lambda = 0.1542$ nm) in the range of 25-100° at room temperature. Magnetic measurements were performed by a vibrating sample magnetometer (VSM - 782 Lake Shore) in an alternating magnetic field with a maximum of 1 kOe at room temperature (300 K). Saturation magnetization (Ms) values were obtained from the high field part of the measured magnetization curves, where the magnetization curve become linear, and line's slop tend to become zero.

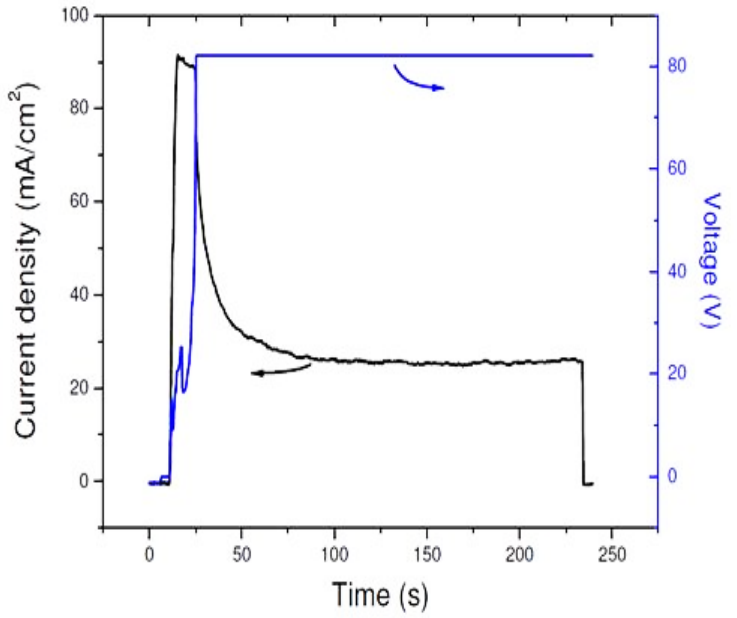

Fig. 1. Current-voltage curve versus time during electropolishing.

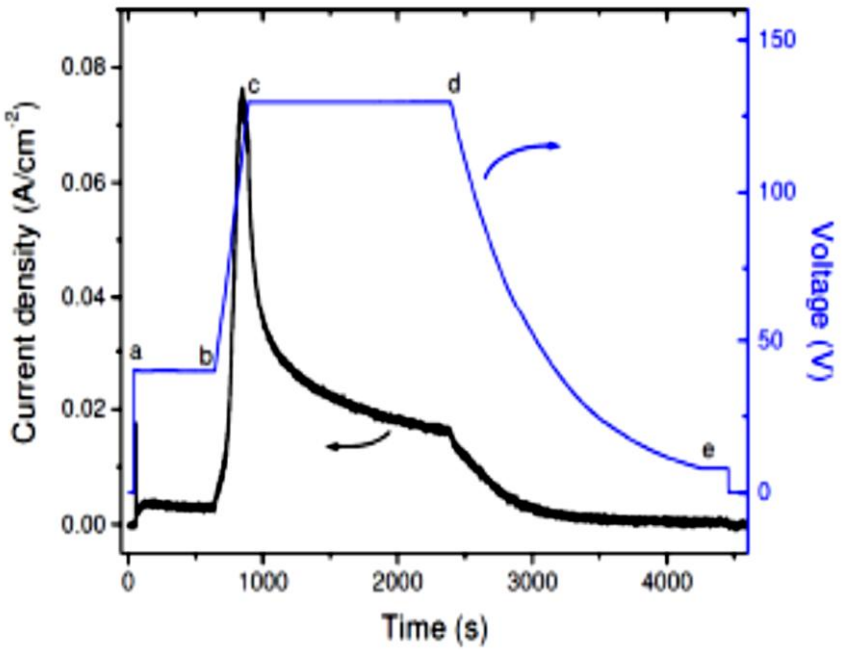

Fig. 2. Current-voltage curve versus time during mild anodizing (a-b), hard anodizing (c-d) and barrier layer thinning (d-e).

3. Results and Discussion

The recorded current changes in Fig. 2 show that first, a lot of currents passed through the sample within 10 minutes, and then the current has dropped as the result of the formation of aluminium oxide on the substrate. Finally, when the formation and dissolution rate of the oxide layer in the barrier layer were equal to each other, the current reached a steady-state [25].

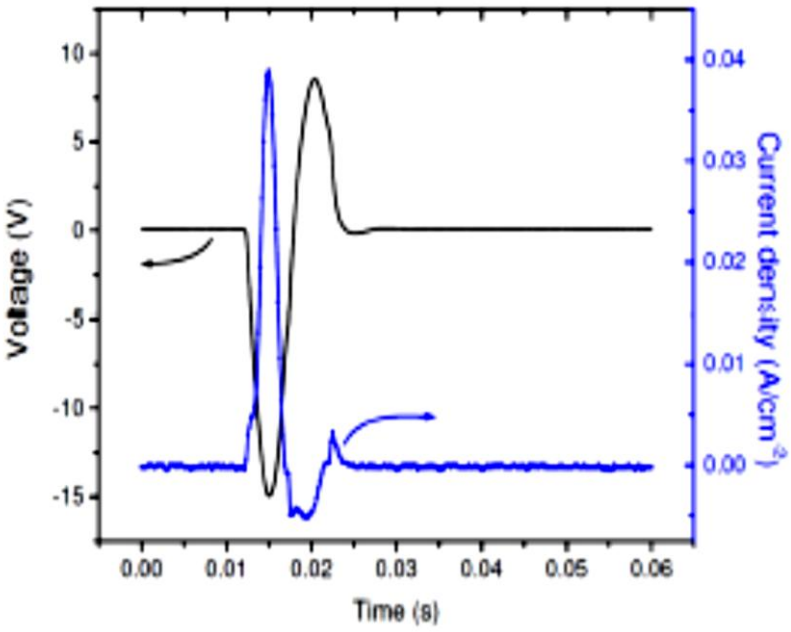

Fig. 3. Current-voltage curve versus time during electrodeposition with applied momentum potential with 50 ms off time.

When the voltage increases more than 40 V, the anodizing current begins to increase gradually. But then, at a certain voltage (about 60 V) the current increases exponentially, and the growth rate will be very high. From this voltage, the process is, in fact, a hard anodizing. During this stage, the growth of alumina is very high, and the depth of pores and the thickness of the barrier layer are increased. With this enhancement in the pores depth and diffusion path length as well as barrier layer thickness, a kind of resistance is created against the anodizing current and ultimately reduces the current [13, 25]. Also, after reaching a voltage of 130 V, the current decreases exponentially due to the higher diffusion length. The sample cross-section at the end of this step is presented in Fig. 4. The thickness of the barrier layer is about 150 nm, which can reduce the quality of electrodeposition due to its insulating nature.

According to Fig. 2 (d-e), by decreasing the voltage, the anodizing current also decreases. The influence of voltage and current decreasing on AAO microstructure are observed in Fig. 5. As shown in Fig. 5, the pores begin to branch out, and their diameter and inter-pore distances are reduced. As an example, the two pores marked with the arrows in this image are approaching each other. During this process, the thickness of the barrier layer is reduced (about 8 nm), and with this thickness, the electrodeposition process is well done.

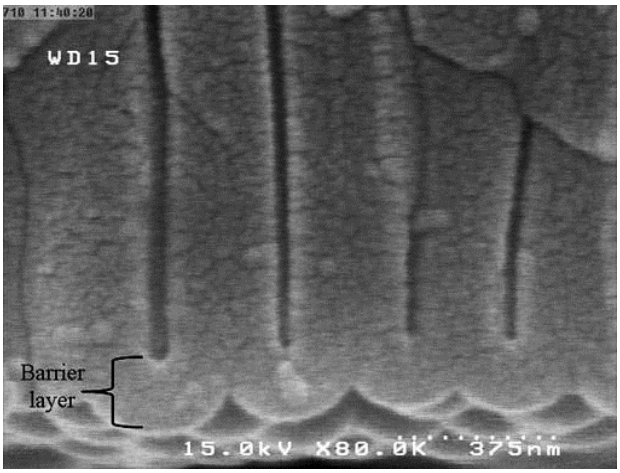

Fig. 4. FESEM image of template cross-section before thinning process.

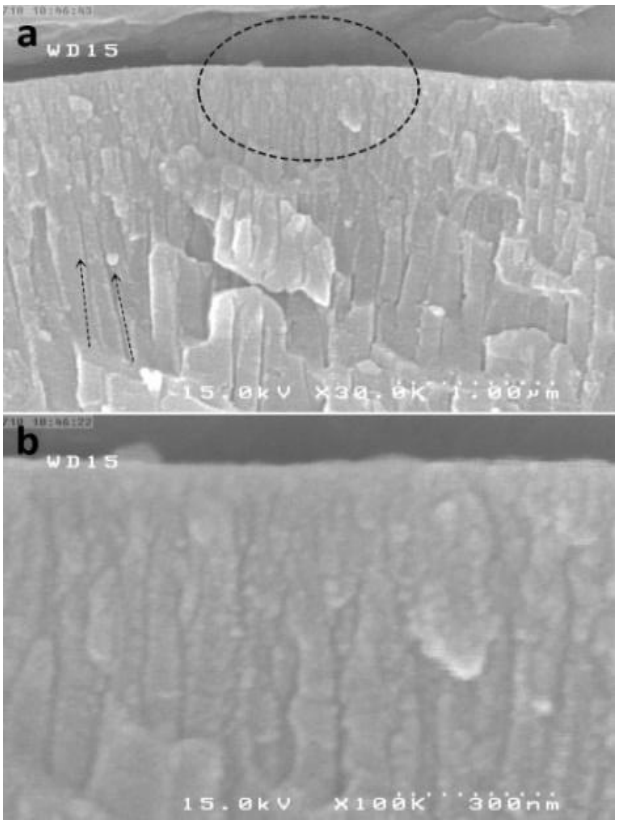

Fig. 5. FESEM image of (a) template cross-section after thinning process, (b) selected area of image a.

Fig. 6 shows the EDS analysis results of AAO formed at the end of the thinning process. It can be seen that the peaks only corresponded to aluminium and oxygen. The results suggest that the AAO was composed of elements Al and O, which related to Alumina formed from anodizing in oxalic acid solution [26].

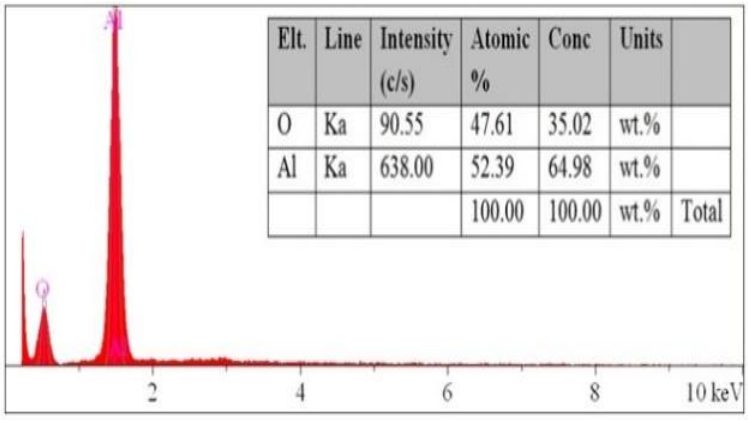

Elt.	Line	Intensity (c/s)	Atomic %	Conc	Units	
O	Ka	90.55	47.61	35.02	wt.%	
Al	Ka	638.00	52.39	64.98	wt.%	
			100.00	100.00	wt.%	Total

Fig. 6. The EDS analysis results of AAO formed on 1100 Al alloy.

By conducting the electrodeposition process, the passed current in the reduction zone is much greater than the oxidation zone, and therefore, in each period, the net deposit charge is much greater than oxidation, and as a result, growth is well done. Nanowires that are grown in alumina can be observed in Fig. 7. The fabricated nanowires can be seen obviously by removing the alumina with the aid of sodium hydroxide solution in order to characterize the nanowires accurately. The diameter of these nanowires is estimated to be about 87 nm, as can be seen in Fig. 8.

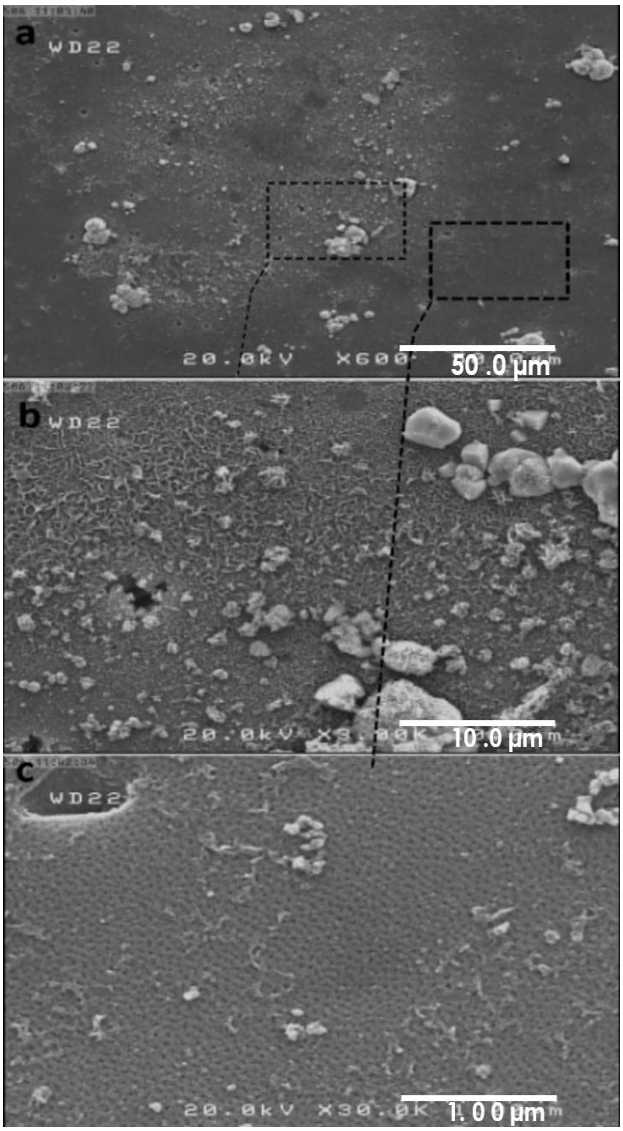

Fig. 7. FESEM images of (a) surface sample, (b) more Co nanowire get out from templates, (c) less Co nanowire get out from templates.

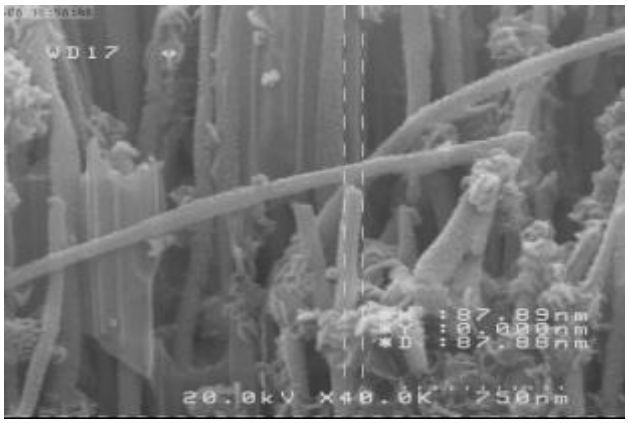

Fig. 8. FESEM image of Co nanowire grown in AAO by electrodeposition process.

According to the results of Fig. 9, which relates to the hysteresis loop of Co nanowire, it can be seen that the coercivity (Hc) value for the nanowires is about 600 Oe, which is several times larger than that of Co bulk. Also, the nanowire's coercivity value even is much larger than that for thin Co layers [27]. In the presence of an external magnetic field, the magnetic moment of the single or multi-domain magnetic materials are also arranged in the direction of the applied field. After removal of the

external magnetic field, remnant magnetization and coercivity will remain in the multi-domain materials, while in single-domain materials, there is no residual magnetization and coercivity due to the rapid return of the magnetic moments to the easy axis [28]. Therefore, thin Co layers have fewer magnetic domains than that of nanowires which have ferri/ferromagnetic behaviour [29]. The saturation (Ms) and remnant magnetization (Mr) in produced nanowires are about 0.081 and 0.04 emu/g, respectively. According to Stoner-Wohlfarth model, the residual ratio (Rs=Mr/Ms) below 0.5 could be characteristic of a single domain nanowires, and for a ratio above 0.5, it means that the nanowires are multi-domain that are randomly oriented [30]. Rs value of fabricated nanowires suggested that these nanowires exhibit ferri/ferromagnetic behavior making them good candidates for a wide range of applications such as MRI, catalytic, photoelectronic, and magnetic recording [31-34]. Moreover, magneto-crystalline anisotropy has a direct relationship with the Rs ratio. It means that the decrease in Mr/Ms ratio can be attributed to the decrease in the magneto-crystalline anisotropy constant [35].

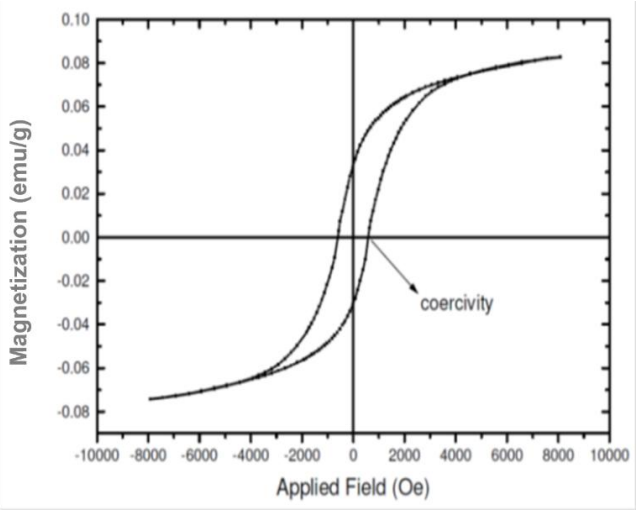

Fig. 9. Hysteresis loops of Co nanowire arrays grown in AAO.

XRD pattern of Co nanowires (Fig. 10) shows that the structural phase of the nanowires is hcp, with peaks at 2θ of 41.7◦, 44.6◦ , and 76.1◦, which are related to the crystalline plates with the orientation of (100), (200) and (110). On the other hand, the peaks of (100) and (110) are related to hcp Co phase formation with the c-axis perpendicular to the wire axis while (002) peak is an indication of hcp Co nanowires with the c-axis parallel to the wire axis. Also, the (101) peak shows c-axis growth is not aligned to the wires axis. Therefore, the crystalline anisotropies and isotropies orientation are not in the same direction, and dual-anisotropies have no constructive effect on each other. It was reported in recent researches that crystalline orientation of (200) causes the improvement of the magnetic properties of prepared nanowires [16, 36].

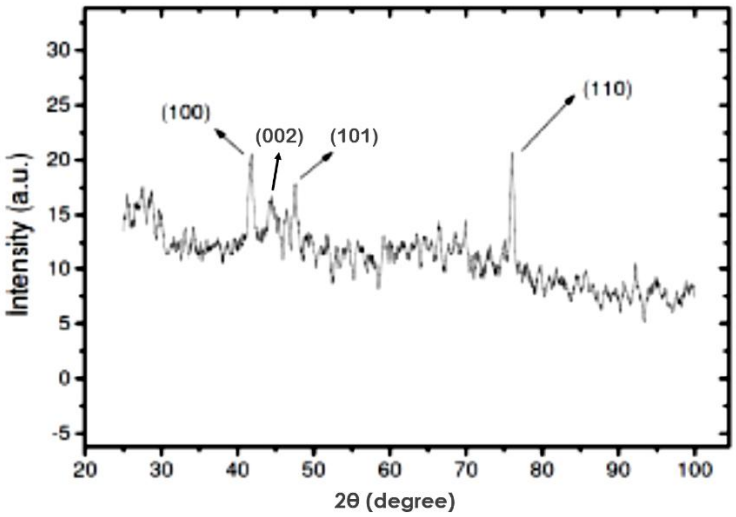

Fig. 10. XRD pattern of Co nanowires.

4. Conclusions

-Fabrication of a suitable template for the electrodeposition process was possible with a hard anodizing (130 volts) after a mild anodizing (40 volts) on 1100 Al alloy.

-By decreasing the voltage at the end of the anodizing process, the thickness of the barrier layer was reduced from about 150 nm to 8 nm. This thickness reduction allowed the electrodeposition to be carried out well.

-The Co nanowires were fabricated using a pulsed electrodeposition process, having a diameter of 87 nm and a hcp structure. The value of coercivity for nanowires is also 600 Oe, which is several times higher than cobalt bulk.

References

[1] S. Goolaup, A. Adeyeye, N. Singh, G. Gubbiotti, "Magnetization switching in alternating width nanowire arrays", Phys. Rev. B, Vol. 75, No. 14, 2007, pp. 14-30.

[2] W. Wu, B. Cui, X.-y. Sun, W. Zhang, L. Zhuang, L. Kong, S.Y. Chou, "Large area high density quantized magnetic disks fabricated using nanoimprint lithography", J. Vac. Sci. Tech. B: Microelectron. Nanometer Struct. Process. Meas. Phenom., Vol. 16, No. 6, 1998, pp. 3825-3829.

[3] R. Skomski, H. Zeng, M. Zheng, D.J. Sellmyer, "Magnetic localization in transition-metal nanowires", Phys. Rev. B, Vol. 62, No. 6, 2000, pp. 3-9.

[4] X. Han, Q. Liu, J. Wang, S. Li, Y. Ren, R. Liu, F. Li, "Influence of crystal orientation on magnetic properties of hcp co nanowire arrays", J. Phys. D: Appl. Phys., Vol. 42, No. 9, 2009, pp. 95005.

[5] K. Maleki, S. Sanjabi, Z. Alemipour, "Ac electrodeposition of Ni-Mn alloy nanowires in aao template", Int. J. Mod. Phys. B, Vol. 29, No. 31, 2015, pp. 155-224.

[6] X.-Y. Lv, J.-W. Hou, Z.-X. Gao, H.-F. Liu, "Synthesis and characteristics of large-area and high-filling cds nanowire arrays in aao template", J. Nanosci. Nanotechnol., Vol. 18, No. 5, 2018, pp. 3709-3712.

[7] P. Wang, L. Gao, L. Wang, D. Zhang, S. Yang, X. Song, Z. Qiu, R.-I. Murakami, "Magnetic properties of feni nanowire arrays assembled on porous aao template by ac electrodeposition", Int. J. Mod. Phys. B, Vol. 24, No. 15, 2010, pp. 2302-2307.

[8] M. Michalska-Domańska, W.J. Stępniowski, L.R. Jaroszewicz, "Characterization of nanopores arrangement of anodic alumina layers synthesized on low-(aa1050) and high-purity aluminum by two-step anodizing in sulfuric acid with addition of ethylene glycol at low temperature", J. Porous Mater., Vol. 24, No. 3, 2017, pp. 779-786.

[9] Y. Choi, J. Hyeon, S. Bu, T. Bae, "Effects of anodizing voltages and corresponding current densities on self-ordering process of nanopores in porous anodic aluminas anodized in oxalic and sulfuric acids", J. Korean Phys. Soc., Vol. 55, No. 2, 2009, pp. 835-840.

[10] W.J. Stępniowski, Z. Bojar, "Synthesis of anodic aluminum oxide (aao) at relatively high temperatures. Study of the influence of anodization conditions on the alumina structural features", Surf. Coat. Technol., Vol. 206, No. 2-3, 2011, pp. 265-272.

[11] T. Aerts, I. De Graeve, H. Terryn, "Study of initiation and development of local burning phenomena during anodizing of aluminium under controlled convection", Electrochim. Acta, Vol. 54, No. 2, 2008, pp. 270-279.

[12] J. Thangthong, S. Prombanpong, "An analysis of burn defect in hard anodized process of al 3003", Adv. Mater. Res., Vol. 1119, 2015, pp. 475.
[13] L. Woo, R. Ji, U. Gösele, K. Nielsch, "Fast fabrication of long-range ordered porous alumina membranes by hard anodization", Nature Mater., Vol. 5, No. 9, 2006, pp. 741.
[14] S. Park, Y.-S. Kim, W.B. Kim, S. Jon, "Carbon nanosyringe array as a platform for intracellular delivery", Nano Lett., Vol. 9, No. 4, 2009, pp. 1325-1329.
[15] J. Zhou, J. He, P. He, H. Zhang, M. Tang, Y. Ji, X. Liu, W. Dang, "Ternary alloy ni–w–p nanoparticles electroless deposited within alumina nanopores", Mater. Sci. Technol., Vol. 24, No. 10, 2008, pp. 1250-1253.
[16] F. Xiu-Xiu, H. Hai-Ning, Z. Shi-Ming, Y. Mao, D. Jun, S. Zhong, "Abnormal temperature dependence of coercivity in cobalt nanowires", Chinese Phys. Lett., Vol. 29, No. 7, 2012, pp. 077802.
[17] J. Chun, J. Lee, "Various synthetic methods for one-dimensional semiconductor nanowires/ nanorods and their applications in photovoltaic devices", Eur. J. Inorg. Chem., Vol. 2010, No. 27, 2010, pp. 4251-4263.
[18] M. Noormohammadi, M. Moradi, "Structural engineering of nanoporous alumina by direct cooling the barrier layer during the aluminum hard anodization", Mater. Chem. Phys., Vol. 135, No. 2, 2012, pp. 1089-1095.
[19] A. Jokar, A. Ramazani, M. Almasi-Kashi, A. Montazer, "The roles of temperature and thickness of barrier layer in the electrodeposition efficiency of nickel inside anodic alumina templates", J. Mater. Sci.: Mater. Elect., Vol. 27, No. 4, 2016, pp. 3995-4002.
[20] M.A. Kashi, A. Ramazani, M. Ghaffari, V. Isfahani, "The effect of growth rate enhancement on the magnetic properties and microstructures of ac electrodeposited co nanowires using non-symmetric reductive/oxidative voltage", J. Cryst. Growth, Vol. 311, No. 21, 2009, pp. 4581-4586.
[21] D. Sellmyer, M. Zheng, R. Skomski, "Magnetism of fe, co and ni nanowires in self-assembled arrays", J. Phys.: Condens. Matter, Vol. 13, No. 25, 2001, pp. R433.
[22] R. Ferre, K. Ounadjela, J. George, L. Piraux, S. Dubois, "Magnetization processes in nickel and cobalt electrodeposited nanowires", Phys. Rev. B, Vol. 56, No. 21, 1997, pp. 14066.
[23] D. Qin, M. Lu, H. Li, "Magnetic force microscopy of magnetic domain structure in highly ordered co nanowire arrays", Chem. Phys. Lett., Vol. 350, No. 1-2, 2001, pp. 51-56.
[24] F. Li, T. Wang, L. Ren, J. Sun, "Structure and magnetic properties of co nanowires in self-assembled arrays", J. Phys.: Condens. Matter, Vol. 16, No. 45, 2004, pp. 8053.
[25] M.A. Kashi, A. Ramazani, M. Noormohammadi, M. Zarei, P. Marashi, "Optimum self-ordered nanopore arrays with 130–270 nm interpore distances formed by hard anodization in sulfuric/oxalic acid mixtures", J. Phys. D: Appl. Phys., Vol. 40, No. 22, 2007, pp. 7032.
[26] C.H. Voon, B.Y. Lim, K. Foo, U. Hashim, S.T. Sam, M.K.M. Arshad, A. Baharuddin, "Effect of concentration of oxalic acid on the synthesis of porous anodic alumina (paa) on aluminum alloy aa6061", Mater. Sci. Forum, 2016, pp. 281.
[27] W. Chen, M. Han, L. Deng, "High frequency microwave absorbing properties of cobalt nanowires with transverse magnetocrystalline anisotropy", Phys. B: Condens. Matter, Vol. 405, No. 6, 2010, pp. 1484-1488.
[28] A. Akbarzadeh, M. Samiei, S. Davaran, "Magnetic nanoparticles: Preparation, physical properties, and applications in biomedicine", Nanoscale Res. Lett., Vol. 7, No. 1, 2012, pp. 144.
[29] Z. Karimi, L. Karimi, H. Shokrollahi, "Nano-magnetic particles used in biomedicine: Core and coating materials", Mater. Sci. Eng. C, Vol. 33, No. 5, 2013, pp. 2465-2475.
[30] J. Das, V.S. Moholkar, S. Chakma, "Structural, magnetic and optical properties of sonochemically synthesized zr-ferrite nanoparticles", Powder Technol., Vol. 328, No. 2018, pp. 1-6.
[31] G. Bertotti, Hysteresis in magnetism: For physicists, materials scientists, and engineers, ed., Academic press, 1998,
[32] C.H. Kim, Y. Myung, Y.J. Cho, H.S. Kim, S.-H. Park, J. Park, J.-Y. Kim, B. Kim, "Electronic structure of vertically aligned mn-doped cofe2o4 nanowires and their application as humidity sensors and photodetectors", J. Phys. Chem. C, Vol. 113, No. 17, 2009, pp. 7085-7090.
[33] C. Pham-Huu, N. Keller, C. Estournes, G. Ehret, M. Ledoux, "Synthesis of cofe 2 o 4 nanowire in carbon nanotubes. A new use of the confinement effect", Chem. Commun., Vol. No. 17, 2002, pp. 1882-1883.
[34] S.M. El-Sheikh, F.A. Harraz, M.M. Hessien, "Magnetic behavior of cobalt ferrite nanowires prepared by template-assisted technique", Mater. Chem. Phys., Vol. 123, No. 1, 2010, pp. 254-259.
[35] V.K. Varadan, L. Chen, J. Xie, Nanomedicine: Design and applications of magnetic nanomaterials, nanosensors and nanosystems, ed., John Wiley & Sons, 2008,

[36] A. Ramazani, M.A. Kashi, G. Seyedi, "Crystallinity and magnetic properties of electrodeposited co nanowires in porous alumina", J. Magn. Magn.Mater., Vol. 324, No. 10, 2012, pp. 1826-1831.